© 2018. Published by The Company of Biologists Ltd | Development (2018) 145, dev162883. doi:10.1242/dev.162883

RESEARCH REPORT

Differentiating cells mechanically limit the interkinetic nuclear migration of progenitor cells to secure apical cytogenesis

Yuto Watanabe*, Takumi Kawaue*,‡ and Takaki Miyata‡

ABSTRACT

Many proliferative epithelia are pseudostratified because of cell cycle-dependent interkinetic nuclear migration (IKNM, basal during G1 and apical during G2). Although most epithelia, including early embryonic neuroepithelia (≤100 µm thick), undergo IKNM over the entire apicobasal extent, more apicobasally elongated (300 µm) neural progenitor cells (radial glial cells) in the mid-embryonic mouse cerebral wall move their nuclei only within its apical (100 µm) compartment, leaving the remaining basal region nucleus-free (fiber-like). How this IKNM range [i.e. the thickness of a pseudostratified ventricular zone (VZ)] is determined remains unknown. Here, we report external fencing of IKNM and the VZ by differentiating cells. When a tight stack of multipolar cells immediately basal to the VZ was 'drilled' via acute neuron-directed expression of diphtheria toxin, IKNM of apicobasally connected progenitor cells continued further towards the basal region of the cell (200 µm). The unfencing-induced basally overshot nuclei stay in S phase for too long and do not move apically, suggesting that external limitation of IKNM is necessary for progenitors to undergo normal cytogenetic behaviors. Thus, physical collaboration between progenitors and differentiating cells, including neurons, underlies brain development.

KEY WORDS: Interkinetic nuclear migration, Radial glia, Ventricular zone, Pseudostratified epithelium, Neocortex, Mouse

INTRODUCTION

Neuroepithelial cells, which are proliferative neural progenitor cells, are elongated to span an ∼100 µm thick brain wall (in early embryonic mice). Their nuclei occupy diverse apicobasal positions, because they move the nucleus and soma in a cell cycle-dependent manner, a process called interkinetic nuclear migration (IKNM) (Sauer, 1935; reviewed in Miyata, 2008; Taverna and Huttner, 2010; Kosodo, 2012; Reiner et al., 2012; Spear and Erickson, 2012; Lee and Norden, 2013). In the neuroepithelium, as in other non-neural thin epithelia (Grosse et al., 2011; Meyer et al., 2011; Ichikawa et al., 2013; Yamada et al., 2013), IKNM occurs throughout the cell (i.e. nuclei move to and from the basal-most region during G1 and G2 phases, respectively). By contrast, more developed primordial brain walls, in which neural progenitor cells (radial glial cells) are more apicobasally elongated (∼300 µm in the mid-embryonic mouse cortex), contain an IKNM-undergoing (pseudostratified) portion only apically [within ∼100 µm, called the ventricular zone (VZ)] (reviewed in Taverna et al., 2014; Miyata et al., 2015; Strzyz et al., 2016; Norden, 2017), with neurons accumulating basally (Fig. 1A).

Currently, the mechanisms by which the range of IKNM (i.e. the thickness of the VZ) is determined and why these ∼300 µm apicobasally elongated mouse cortical progenitor cells do not send their nuclei basally beyond 100 µm remain unknown. Progenitor cells themselves might limit the basal extent of IKNM, possibly based on a cell-intrinsic measurement of the time of basal nucleokinesis and/or the distance of nuclear displacement from the apical surface (Fig. 1B). It is also possible that the basal IKNM limit is determined extrinsically, in particular physically, by an external layer called the subventricular zone (SVZ) (Fig. 1C). Because the cortical VZ is subject to physiological crowding, and is consequently under mechanical load (Okamoto et al., 2013; Saito et al., 2018; Shinoda et al., 2018), it could interact mechanically with differentiating cells, including the youngest 'premigratory' neurons and their parent intermediate progenitors that are densely stacked for a transient (12-24 h) stay in the SVZ (Shoukimas and Hinds, 1978; Takahashi et al., 1996; Tabata and Nakajima, 2003; Haubensak et al., 2004; Miyata et al., 2004; Noctor et al., 2004; Ochiai et al. 2009). To investigate a potential mechanical role of the SVZ, we 'drilled' holes into it and assessed the behavior of the progenitor cells whose nuclei and somata constitute the VZ.

RESULTS AND DISCUSSION

SVZ can be locally drilled via *in utero* electroporation-mediated acute ablation of differentiating cells

As the first step for investigating whether the VZ is mechanically fenced by the SVZ, *in utero* electroporation (IUE) was carried out on mouse cerebral walls at embryonic day (E) 12 with a vector for expression of the diphtheria toxin A chain (DTA) under the control of the *NeuroD* promoter, which is expected to be most active in the SVZ (Schwab et al., 1998; Hevner et al., 2006) (NeuroD-DTA). Our immunohistochemistry showed that the SVZ, when visualized as a dense stack of nuclei positive for Tbr2 (also called Eomes), contained neurons that were NeuroD$^+$ (132/150, 88%), p27$^+$ (161/210, 77%) and Ki67$^-$ (92/138, 67%) (Fig. S1A-C), and intermediate (basal) progenitors (NeuroD$^-$, p27$^-$, Ki67$^+$). NeuroD-DTA IUE resulted in acute (within 12 h) and SVZ-specific cytotoxicity, as revealed by immunostaining for cleaved caspase 3 (Fig. 1D). Both neurons and intermediate progenitors were ablated (Fig. S1D). At 24 h after IUE, the density of Tbr2$^+$ nuclei in the SVZ was clearly reduced (Fig. 1E). To investigate the possible role of the SVZ as a physical barrier, we compared the intact SVZ with the DTA-introduced SVZ using Gadd45g-d4Venus transgenic mice (Kawaue et al., 2014), in which the somata and processes of all SVZ cells can be exclusively visualized, allowing all cellular components to be observed [SVZ-forming Tbr2$^+$ cells are all Gadd45g-d4Venus$^+$ (Kawaue et al., 2014)]. Both coronal and horizontal

Department of Anatomy and Cell Biology, Nagoya University Graduate School of Medicine, 65 Tsurumai, Showa, Nagoya 466-8550, Japan.
*These authors contributed equally to this work

‡Authors for correspondence (tmiyata@med.nagoya-u.ac.jp; kawaue@med.nagoya-u.ac.jp)

T.K., 0000-0002-8600-7734; T.M., 0000-0002-5952-0241

Received 24 December 2017; Accepted 7 June 2018

Development (2018) 145, dev162883. doi:10.1242/dev.162883

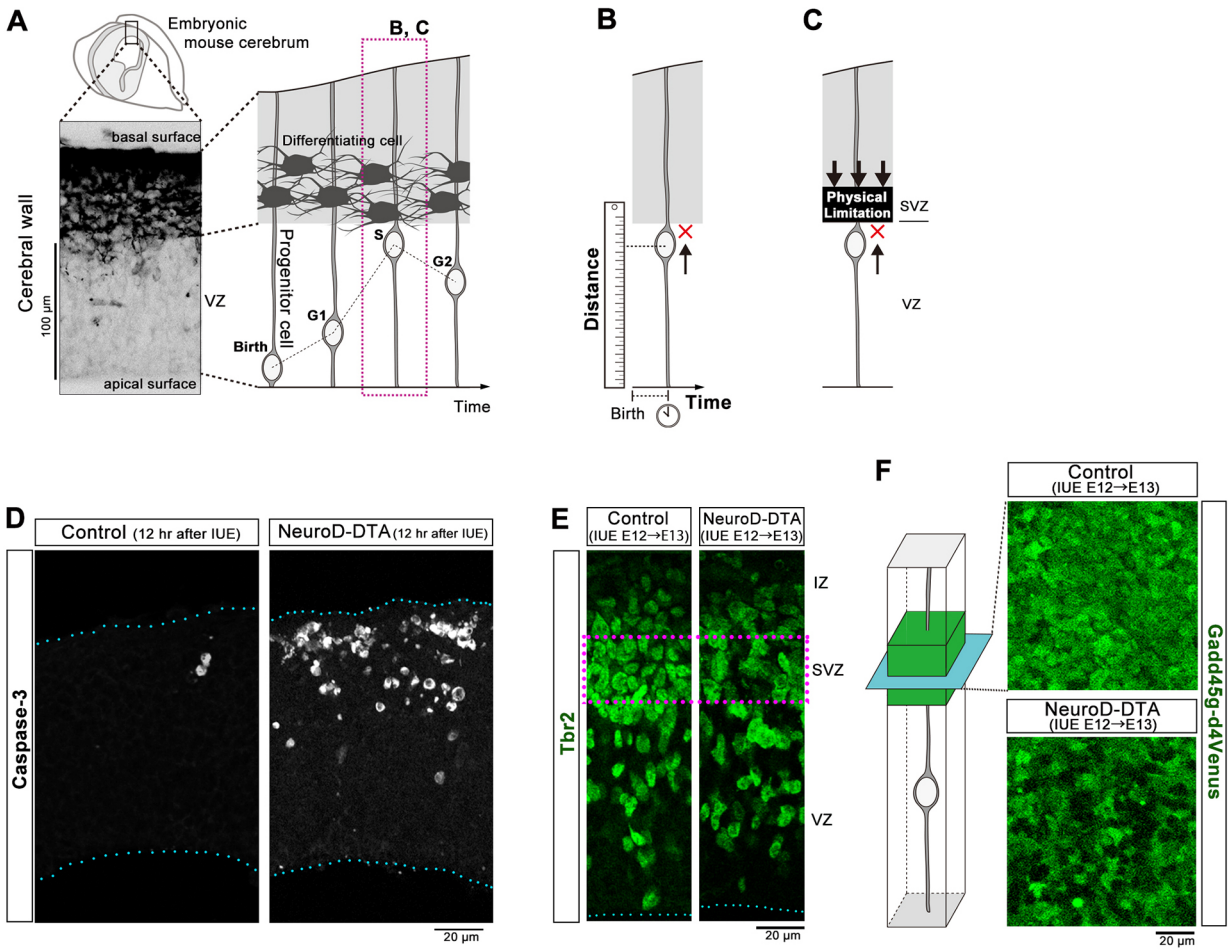

Fig. 1. IUE-mediated acute 'drilling' of the SVZ consisting of differentiating cells. (A) Schematic illustration of the embryonic mouse cerebral wall. Anti-βIII tubulin immunostaining (left) shows that the VZ (~100 µm thick), in which IKNM of progenitor cells (right panel) occurs, is basally neighbored by an accumulation of multipolar-shaped neurons. (B,C) Two hypotheses that might explain how IKNM range is determined: progenitor cells could intrinsically measure the time of basal nucleokinesis and/or the distance of nuclear displacement from the apical surface (B), and/or differentiating cells could physically limit progenitor cell IKNM (C). (D) Cell death detected with anti-caspase 3 12 h after IUE with pCAG-EGFP-3NLS (control) or pNeuroD-DTA at E12. (E) Anti-Tbr2 immunostained coronal sections of E13 cerebral walls, showing that there were significantly fewer Tbr2$^+$ cells in the SVZ after NeuroD-DTA IUE than in the control (P=4.5×10^{-9}, two-tailed t-test, n=11). (F) Horizontal section two-photon microscopic images of the SVZ in E13 Gadd45g-d4Venus mice, showing that d4Venus$^+$ cells (i.e. differentiating cells forming the SVZ) were sparse in the NeuroD-DTA-introduced cerebral wall. IZ, intermediate zone; SVZ, subventricular zone; VZ, ventricular zone.

sectional microscopy revealed that, whereas the normal SVZ is homogeneously filled with Gadd45g-d4Venus$^+$ elements with no obvious holes, the NeuroD-DTA-expressing SVZ had massive Gadd45g-d4Venus$^-$ regions, indicating successful acute drilling of the SVZ (Fig. 1F; Fig. S2A).

SVZ drilling resulted in overshooting of basal IKNM by apicobasally spanning progenitor cells in a VZ volume-dependent manner

The Gadd45g-d4Venus$^-$ intra-SVZ spots that emerged by E13 following introduction of NeuroD-DTA at E12 were filled with Sox2$^+$ nuclei (Fig. 2A). The emergence of extra-VZ Sox2$^+$ nuclei correlated with the degree of IUE (as assessed by the number of GFP$^+$ cells per field) (Fig. 2B; Fig. S2B). These results suggested that the nuclei and somata of the undifferentiated VZ cells may have 'popped out' (been displaced) into the neuron-deprived SVZ after the killing of differentiating cells (by 12 h) but before our observation of the SVZ (at 24 h after IUE) (Fig. 2C). To directly observe such overshooting of nuclei and somata undergoing IKNM from the VZ into the SVZ, we live-monitored Lyn-mCherry-labeled progenitor cells that spanned the apicobasal surfaces of cultured slices. As shown in Fig. 2D (Movie 1), we frequently observed that the nuclei and somata of these cells moved further than 100 µm from the apical surface, and therefore into the SVZ. In slices prepared from Gadd45g-d4Venus mice, we observed that the Lyn-mCherry-labeled soma of a highly elongated progenitor cell moved into, and even more basally than, the Gadd45g-d4Venus$^+$ zone (i.e. the SVZ) through a tunnel-like d4Venus$^-$ region (Fig. 2E). When we introduced EF1α-DTA into the VZ, some VZ cells died, but many others (un-electroporated cells), including those that immediately neighbored the caspase 3$^+$ dying VZ cells, survived, maintaining the pseudostratified structure of VZ as overall normal (though cell density was slightly decreased), with no overshooting phenotype (data not shown). This control ablation experiment suggests that the nuclear/somal 'popping out' observed by NeuroD-DTA IUE was not due to DTA toxicity to progenitor cells.

Can this overshooting phenotype be explained by the fact that the SVZ chemically limits basal IKNM? If such a chemical barrier were the main mechanism, the nuclear overshooting that was seen in Fig. 2A would not have been observed. Because of diffuse, rather than focal, electroporation, many Gadd45g-d4Venus$^+$ SVZ cells

Development (2018) 145, dev162883. doi:10.1242/dev.162883

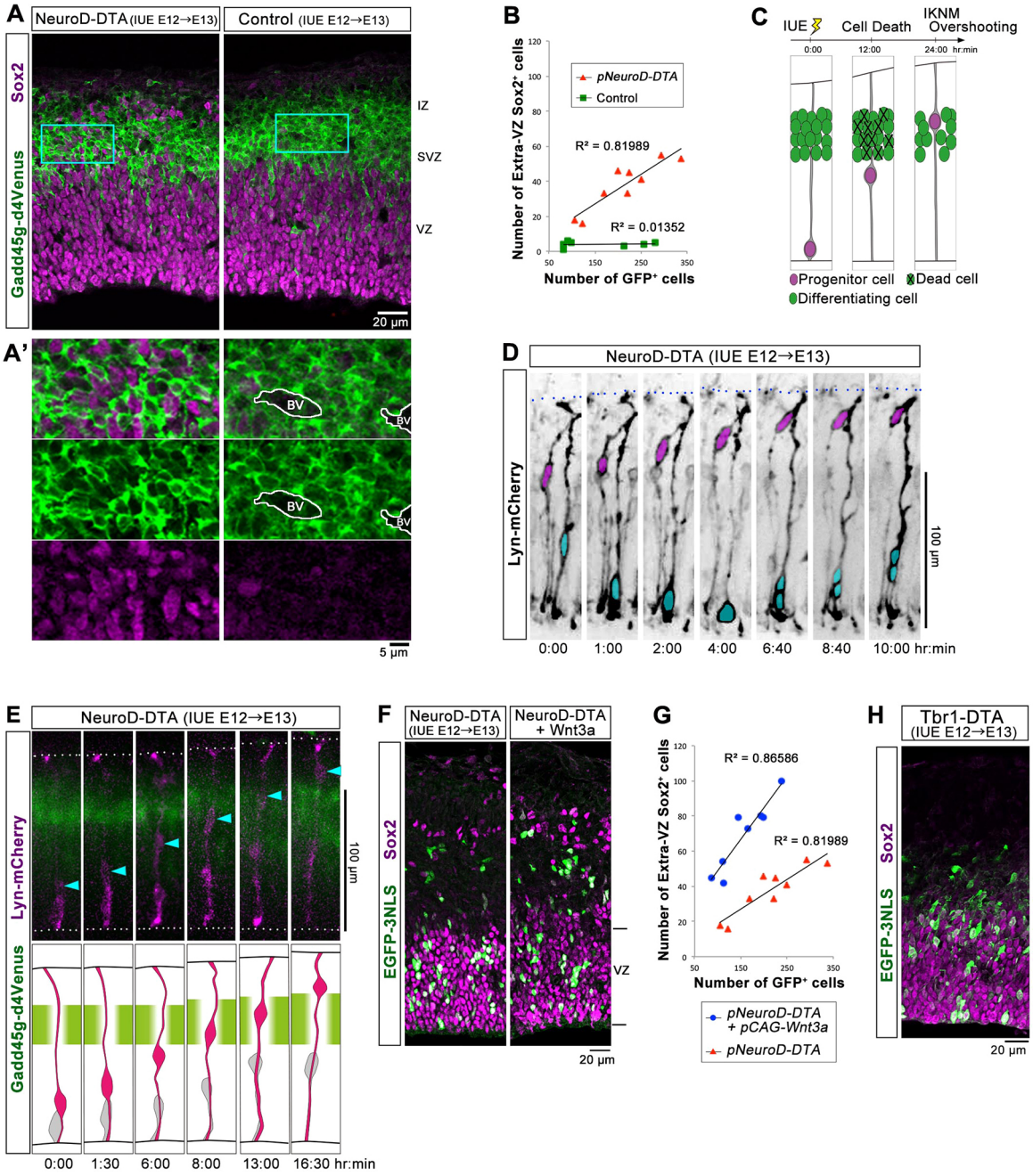

Fig. 2. NeuroD-DTA IUE at E12 results in the basal overshooting of IKNM by E13. (A,A′) Anti-GFP and anti-Sox2 double immunostaining showing that NeuroD-DTA-mediated acute SVZ drilling induced extra-VZ Sox2$^+$ nuclei. BV, blood vessel. (B) Graph shows the relationship between the number of GFP$^+$ cells per field and the number of extra-VZ Sox2$^+$ nuclei (see also Fig. S2B). Regression lines (black) and results of statistical analysis are shown (n=9 for NeuroD-DTA, n=7 for control). (C) Schematic illustration to interpret the *in vivo* result of NeuroD-DTA-induced extra-VZ Sox2$^+$ nuclei. (D) Time-lapse observation of abnormally too basal IKNM (magenta) shown by a progenitor-like cell. Another progenitor cell nucleus/soma (cyan) showed apical IKNM to subsequently undergo mitosis, indicating healthiness of the cultured slice. (E) Time-lapse observation of a Lyn-mCherry-labeled progenitor-like cell in a slice prepared from a Gadd45g-d4Venus mouse cerebral wall that had been electroporated with NeuroD-DTA migrating through a 'drilled' region of the Gadd45g-d4$^+$ SVZ. (F,G) VZ proliferation-enhancing Wnt3a significantly increased NeuroD-DTA-induced extra-VZ Sox2$^+$ nuclei (P=0.0081, ANCOVA, n=9). (H) Introduction of Tbr1-DTA to kill post-migratory neurons basal to the SVZ did not produce extra-Sox2$^+$ nuclei.

still existed with multiple, but small (~5 μm diameter), holes in the SVZ. In this situation, the loss of hypothetical chemical repellants from a given dying SVZ cell would have easily been compensated for by the surrounding SVZ cells, the majority of which survived. To study whether loosening of the SVZ without killing cells leads to the overshooting phenotype, we used a method described by Yoshinaga et al. (2012). This involved acute sequestration of Ena/VASP family proteins (working downstream of the actin-remodeling protein lamellipodin) from the plasma membrane of SVZ cells, via IUE with an expression vector for a fusion protein of the FP4 motifs and a mitochondrial targeting signal (FP4-mito). This reduces the primary processes extended from SVZ cells, probably weakening a physical barrier. As expected, many ectopic Sox2$^+$ nuclei were found in the SVZ of E13 cerebral walls following

Development (2018) 145, dev162883. doi:10.1242/dev.162883

FP4-mito IUE at E12 (Fig. S2C). Thus, although we do not completely exclude the possibility of a chemical contribution of the SVZ to limiting basal IKNM, mechanical limitation is much more likely.

Both $Sox2^+$ nuclei of progenitor cells that were directly electroporated (GFP^+ or $mCherry^+$) and those of reporter-negative cells exited the VZ (Fig. 2F). Accordingly, we sought to determine whether an experimental increase in the VZ volume would enhance the emergence of the heterotopic (more basal) $Sox2^+$ nuclei. To investigate this, we co-electroporated Wnt3a, which induces over-proliferation of early cortical progenitor cells and increases compressive and/or expansive stress in the VZ (Okamoto et al., 2013). The number of extra-VZ $Sox2^+$ nuclei was significantly greater in samples treated with NeuroD-DTA+Wnt3a than in those treated with NeuroD-DTA alone (ANCOVA, P=0.0081, n=9) (Fig. 2F,G; Fig. S2B). This observation suggests that intra-VZ pressure may have been responsible for the overshooting of $Sox2^+$ nuclei, supporting a model in which the SVZ normally plays a mechanical role in fencing the pressurized VZ.

In a previous study (Brockschnieder et al., 2004), Nex-Cre mice were crossed with the Rosa26LacZ/DT-A mice, and cortical neurons were ablated as early as E12, leading to a 'wave-like structure' emerging from the VZ at E18. In another study, in which $Dbx1^{loxP\text{-}stop\text{-}loxP\text{-}DTA}$ mice were crossed with *Nestin:Cre* mice (Freret-Hodara et al., 2017), the authors observed neuronal death from E12 followed by extra-VZ $Pax6^+$ or $Sox2^+$ nuclei at E14. These findings are consistent with our observations and suggest that the aforementioned phenotype we obtained may not be specific to the use of NeuroD-DTA. Indeed, we obtained the same phenotype when DTA-dependent ablation was performed using the *Gadd45g* promoter at E12 (data not shown). Importantly, however, expression of DTA under the *Tbr1* promoter, which is expected to be active in regions more basal than the SVZ (Hevner et al., 2006), and indeed killed cells in such regions (Fig. S2D) by 24 h, did not result in the basal 'popping out' of $Sox2^+$ nuclei until 24 h (Fig. 2H) and 48 h (Fig. S2E), suggesting that drilling of the SVZ (i.e. physical unfencing of the VZ) was crucial to the basal overshooting of $Sox2^+$ nuclei.

Basally overshot nuclei and somata induced by VZ unfencing do not turn back, even though the apical process remains intact

Does the overshooting of nuclei and somata to the SVZ or beyond affect the behavior of progenitor cells? To answer this question, and thus address the biological role of the normal SVZ fence formed by differentiating cells, we analyzed embryos electroporated with NeuroD-DTA at E12 at a later time point (48 h after IUE, at E14). First, we found that the extra-VZ $Sox2^+$ nuclei remained and were more basally distributed (Fig. 3A). This result was reproduced when embryos were electroporated with NeuroD-DTA at E13 and analyzed at E15 (data not shown). The cells containing such extra-VZ $Sox2^+$ nuclei had much longer (~200 µm) apical processes (Fig. 3B; Fig. S3A) than progenitors in normal E14 cerebral walls (~100 µm) or those in NeuroD-DTA-expressing cerebral walls at 24 h after IUE (E13) (~130 µm). This suggests that if the distance between the nucleus/soma and the apical surface (i.e. the length of the apical process) increases above a threshold, as may have occurred in cells that have lost the SVZ fence, progenitor cells cannot undergo the normal nuclear/somal movement towards the apical surface. To directly test this possibility, we live-monitored progenitor cells with abnormally long (~200 µm) apical processes, and found that they did not move their nucleus and soma over the course of 24 h (Fig. 3C, Movie 2). This observation supports our model that the physical fencing of the VZ by the SVZ, and the resultant maintenance of appropriate apical-process length, are required for progenitor cells to undergo normal apicalward IKNM. The inability of overshot nuclei to undergo apical movement could partly be explained by insufficiency of dynein-related molecules normally enriched near the apical surface (Hu et al., 2013). Possible intracellular compartmentalization, such as that shown in *Drosophila* neurons (Katsuki et al., 2009), should be studied in IKNM-undergoing progenitor cells. The nucleus-overshot progenitor cells remained until at least E16 (Fig. S3B).

S phase is prolonged in progenitors whose nuclei and somata basally overshoot and do not return apically

It is also possible that abnormal cell cycle progression in the apically connected progenitor cells affects nucleokinesis. It is known that

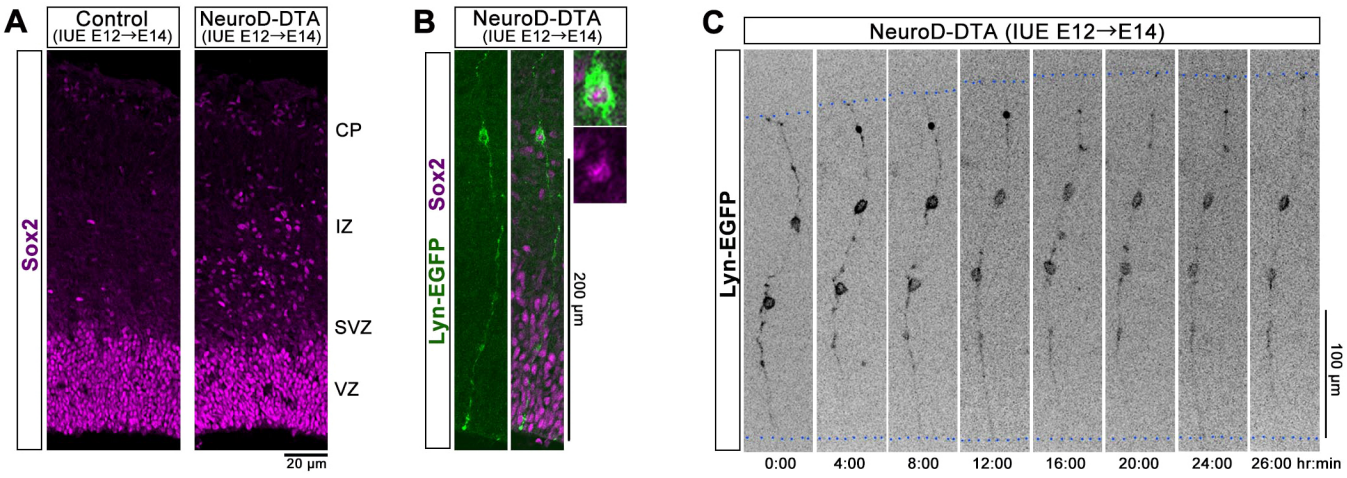

Fig. 3. Extra-VZ $Sox2^+$ nuclei induced by VZ unfencing exist more basally in E14 cerebral walls than at E13. (A) Anti-Sox2 immunostaining showing extra-VZ $Sox2^+$ nuclei in E14 cerebral walls that had been electroporated with control or NeuroD-DTA vectors at E12. CP, cortical plate; IZ, intermediate zone; SVZ, subventricular zone; VZ, ventricular zone. (B) Anti-Sox2 and anti-GFP double immunostaining showing an example of the apically connected Sox2-expressing progenitor cells. (C) Time-lapse observation of two apically connected progenitor-like cells whose nuclei and somata were outside the VZ. Both cells did not move the nucleus and soma to the apical surface (bottom). Blue dotted lines, apical (bottom) and basal surfaces.

Development (2018) 145, dev162883. doi:10.1242/dev.162883

apical IKNM is dependent on the normal entrance of VZ cells into G2 phase (Ueno et al., 2006; Kosodo et al. 2011; Leung et al., 2011). To directly monitor cell cycle progression in progenitor cells whose nuclei overshot (~200 µm), we electroporated Fucci (mAG-hGem) transgenic mice, in which cells in S/G2 phase emit green fluorescence (Sakaue-Sawano et al., 2008), with NeuroD-DTA, EF1α-Cre and EF1α-Lyn-mCherry at E12, and then performed time-lapse observations of Lyn-mCherry-labeled progenitor cells in slices prepared at E14. In the VZ, mAG^{+} nuclei/somata were widely observed from a basal (50-90 µm) VZ region (which contained the nuclei/somata of S-phase cells) to a region near the apical surface (Fig. 4A), and many of them moved to the apical side with gradually increasing mAG intensity (between 'F_{begin}' and 'F_{max}' in Fig. 4B). This reflected successful completion of S phase and progression through G2 phase. Subsequently (after 'F_{max}' in Fig. 4B), the mAG intensity near and/or at the apical surface decreased, and the cells soon became mAG^{-}, indicating completion of M phase (schematically illustrated in Fig. 4A). By contrast, we observed that the extra-VZ (non-migratory) somata of apically connected progenitor cells continued to be moderately mAG^{+}, but the level of mAG did not increase, as is normally observed during G2 phase, for up to 24 h (Fig. 4C). Similar nuclei with low and stable (non-increasing) mAG intensity were observed frequently outside the VZ (Fig. 4B,D).

In vivo experiments were performed to investigate the possibility of S-phase prolongation and/or arrest, which was suggested from the

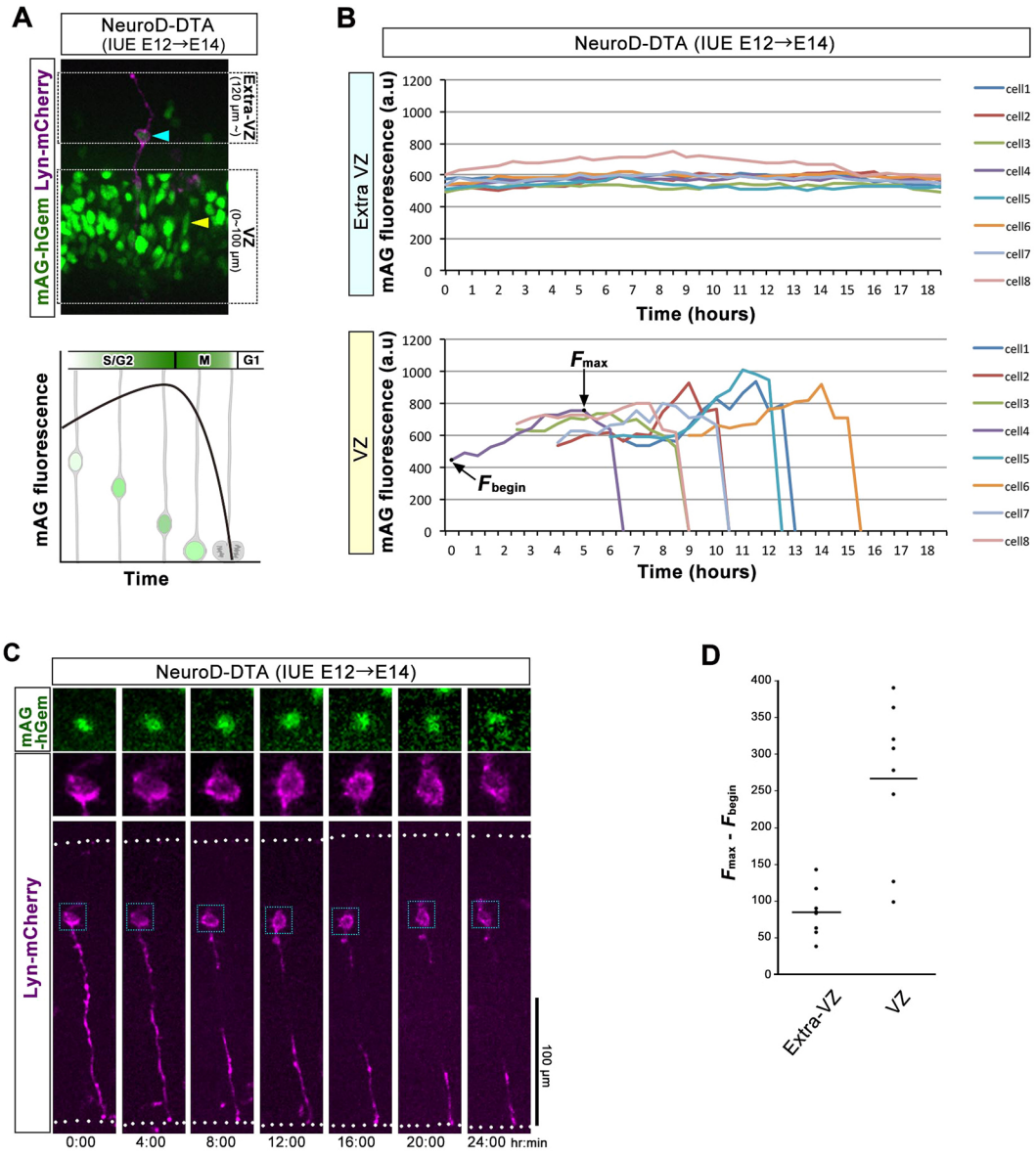

Fig. 4. Live assessment of S-G2 progression using Fucci (mAG-hGem) cerebral wall slices. (A) Live observation of a cerebral wall slice prepared from an E14 Fucci transgenic mouse that had been electroporated with NeuroD-DTA at E12 (upper panel). mAG^{+} nuclei were seen in the VZ (yellow arrowhead), schematically illustrated in the lower panel, and outside the VZ (cyan arrowhead). (B) Comparative time series of mAG fluorescence of progenitor cell nuclei and somata in the VZ and those outside the VZ. Although mAG fluorescence in the VZ nuclei gradually increased, reflecting progression of G2 phase, mAG fluorescence of the extra-VZ nuclei remained almost constant. (C) Time-lapse observation of an apically connected progenitor-like cell whose nucleus was outside the VZ and only moderately mAG^{+}. White dotted lines: apical (bottom) and basal surfaces. (D) Graph summarizing time courses of mAG intensity. The mean (horizontal line) and individual data points are shown. Subtractions of fluorescence intensity at the beginning of observation (F_{begin}) from the maximal mAG-fluorescence (F_{max}) were significantly greater in the intra-VZ nuclei than the extra-VZ nuclei (P=0.0014, two-tailed t-test, n=8).

Development (2018) 145, dev162883. doi:10.1242/dev.162883

Fucci assays. We compared the labeling index (LI) between the normal intra-VZ ($Ki67^+$) nuclei and the NeuroD-DTA-induced extra-VZ $Ki67^+$ nuclei 30 min after BrdU administration. If S-phase progression had indeed been impaired, DNA replication would not finish and the LI would increase (Duronio et al., 1998; Estivill-Torrus et al., 2002). We found that the BrdU LI was significantly greater in the extra-VZ $Ki67^+$ nuclei that had been induced by NeuroD-DTA IUE than in the intra-VZ nuclei of cerebral walls electroporated with control or NeuroD-DTA vectors (Fig. S4A,B). These results together suggest prolongation and/or arrest of S phase in progenitor cells whose nuclei and somata had 'popped out' from the VZ. As the contribution of apically localized molecules such as atypical protein kinase C (Sabherwal et al., 2014) to cell cycle control have been reported, the 'popped-out' nuclei might have suffered from unavailability of such cell cycle-promoting intracellular factors (Fig. S4C).

In summary, acute SVZ-targeting ablation of differentiating cells resulted in the overshooting of basal IKNM in apically connected progenitor cells (to a depth of ∼200 µm from the apical surface), in addition to secondary failures in cell-cycle progression and apical IKNM by these cells (Fig. S4C). Therefore, a mechanical collaboration between progenitor cells and differentiating cells, including premigratory neurons, defines the basal range of IKNM and the thickness of the VZ (normally ∼100 µm), thereby aiding the 3D dynamics and cytogenesis at the apical surface of progenitor cells. Although an ∼200 µm long apical process is abnormal for progenitor cells in the mid-embryonic mouse cerebral wall, it is normal in the human neocortical VZ, which can be 200 µm thick (Zecevic, 1993). Therefore, this study establishes a basis for future comparative studies aimed at elucidating the molecular mechanisms that enabled the range of IKNM to be extended by 100 µm from mouse to human.

MATERIALS AND METHODS

Animal

The animal experiments were conducted according to the Japanese Act on Welfare and Management of Animals, Guidelines for Proper Conduct of Animal Experiments (published by the Science Council of Japan) and the Fundamental Guidelines for Proper Conduct of Animal Experiment and Related Activities in Academic Research Institutions (published by the Ministry of Education, Culture, Sports, Science and Technology, Japan). All protocols for animal experiments were approved by the Animal Care and Use Committee of Nagoya University (No. 29006). Pregnant female mice (*Mus musculus*) were obtained from SLC (Hamamatsu, Japan; for ICR mice) or by mating in Nagoya University. Mice used were Gadd45g-d4Venus transgenic mice (accession number CDB0490T at www2.clst.riken.jp/arg/TG%20mutant%20mice%20list.html; Kawaue et al., 2014) and Fucci mice (Fucci S/2G/M-Green#504, accession number RBRC02706; www2.brc.riken.jp/lab/animal/detail.php?brc_no=;RBRC02706&lang=en Sakaue-Sawano et al., 2008). E0 was defined as the day of vaginal plug identification.

Plasmids

The pNeuroD-DTA, pGadd45g-DTA, pTbr1-DTA and pEF1α-DTA were constructed using pBlue-DTA [a gift from Mitsuhiro Hashimoto (Fukushima Medical University, Fukushima, Japan), constructed using pMC1DTApA (Araki et al., 2006)], pNeuroD-cre [a gift from Tamar Sapir (Weizmann Institute, Rehovot, Israel) (Sapir et al., 2008)], pGadd45 *g* 5′ flanking (Kawaue et al., 2014), pTbr1 5′ flanking [a gift from Carina Hanashima (Waseda University, Tokyo, Japan) (Toma et al., 2014)] or pEF1α-Neurog2 (Kawaue et al., 2014). The pCAG-EGFP-FP4-mito and pCAG-EGFP-AP4-mito were kind gifts from Kazunori Nakajima (Keio University, Tokyo, Japan) (Yoshinaga et al., 2012). Given the fact that the Ena/VASP family proteins specifically bind to the FP4 (FPPPP) motifs of lamellipodin, we used an expression vector of a fusion protein of the FP4 motifs and a mitochondrial targeting signal (FP4-mito) to sequester the Ena/VASP family proteins into the mitochondria. As the negative control, we used an AP4-mito, in which a phenylalanine residue of each motif was changed to an alanine residue. For sporadic labeling of progenitor cells, pEF1α-LPL-Lyn-mCherry was constructed using pSico-mCherry and pEF1α-LPL-Lyn-EGFP (Okamoto et al., 2013) and co-electroporated with pEF1α-Cre (Okamoto et al., 2013). The reporter plasmid vectors used were: pCAG-EGFP-3NLS (Figs 1D-F and 2A,B,F-H, Figs S1, S2B,D,E and S4A,B), pEF1α-LPL-Lyn-EGFP (Fig. 3A-C, Figs S2C and S3) and pEF1α-LPL-Lyn-mCherry (Figs 2D,E, 4A-D and Fig. S2A).

In utero electroporation

Pregnant female mice were anesthetized by an intraperitoneal injection of pentobarbital sodium (75 µg/g). After injection of DNA solutions (1 µg/µl of pNeuroD-DTA, pGadd45g-DTA, pTbr1-DTA, pEF1α-DTA, pCAG-EGFP-FP4-mito or pCAG-EGFP-AP4-mito; 0.5 µg/µl of pEF1α-LPL-Lyn-EGFP, pEF1α-LPL-Lyn-mCherry or pCAG-EGFP-3NLS; and 0.001 µg/µl of pEF1α-Cre) into the lateral ventricle, the head of the embryo in the uterus was placed between the discs of a forceps-type electrode (disc electrodes of 3 mm; Nepa Gene, CUY650P3) and electric pulses (24V) were given three times.

Immunohistochemistry

The brains were fixed using periodate-lysine-paraformaldehyde (PLP) fixative, immersed in 20% sucrose, embedded in OCT compound (Miles Laboratories), and then frozen and sectioned coronally (16 µm). Frozen sections were treated with the following primary antibodies: anti-Pax6 (rabbit, Covance, PRB-278P, 1:300); anti-Sox2 (rabbit, Abcam, ab97959, 1:500); anti-Ki67 (mouse, Novocastra Laboratories, NCL-L-Ki67-MM1, 1:200); anti-Tbr2 (Eomes) (rabbit, Abcam, ab23345, 1:500); anti-pH3 (rabbit, Millipore, 06-570, 1:300); anti-BrdU (rat, Novus Biologicals, NB500-169, 1:2000); anti-cleaved caspase 3 (rabbit, Cell Signaling, #9661, 1:500); anti-βIII-tubulin (mouse, Covance, MMS-435P, 1:1000); anti-p27 (mouse, BD Biosciences, 610241, 1:500); anti-NeuroD (goat, Santa Cruz Biotechnologies, sc-1084, 1:100); or anti-GFP (rat, Nacalai Tesque, 04404-84, 1:500; rabbit, MBL International Corporation, 598, 1:500; chick, Aves Labs, GFP-1020, 1:500). After washes, sections were treated with Alexa Fluor 488-, Alexa Fluor 546- or Alexa Fluor 647-conjugated secondary antibodies (Thermo Fisher Scientific, A-11029, A-11006, A-11034, A-11030, A-11035, A-11081, A-21236, A-21245, 1:200), and subjected to confocal microscopy using an Olympus FV1000.

Live observation in slice culture

Slice cultures were prepared as described previously (Miyata et al., 2001; Kawaue et al., 2014). Briefly, cerebral walls were coronally sliced (200-300 µm) manually and mounted in dishes using collagen gel (AteloCell IAC-30, Koken), and cultured in DMEM/F12 containing horse serum (5%), fetal bovine serum (5%), N2 supplement (Gibco, 1:100), EGF (PeproTech, 10 ng/ml) and bFGF (Invitrogen, 10 ng/ml). Time-lapse confocal microscopy was performed using an upright CSU-X1 microscope (Yokogawa) equipped with an iXon+ CCD camera (Andor). Chambers for on-stage culture were filled with 40% O_2. Horizontal sectional observations at the level of the SVZ were performed on freshly isolated cerebral walls (400-500 µm×400-500 µm) using a two-photon microscope (AiRMP, Nikon). For imaging in slices prepared from Fucci mice, comparative time series of mAG fluorescence of progenitor cell nuclei and somata in the VZ and those outside the VZ were taken (measured by ImageJ and expressed as arbitrary units).

Acknowledgements

We thank Satoshi Yoshinaga and Kazunori Nakajima for providing vectors and valuable comments on multipolar cells; Atsushi Miyawaki for Fucci mice; Tamar Sapir, Mitsuhiro Hashimoto and Carina Hanashima for plasmids; Namiko Noguchi, Kumiko Ota, Maiko Kuroda and Makoto Masaoka for excellent technical assistance; and members of Miyata laboratory for discussion.

Competing interests

The authors declare no competing or financial interests.

Author contributions

Conceptualization: T.K., T.M.; Methodology: Y.W., T.K., T.M.; Validation: Y.W., T.K., T.M.; Formal analysis: Y.W., T.K., T.M.; Investigation: Y.W., T.K., T.M.; Resources:

T.K.; Data curation: Y.W., T.K., T.M.; Writing - original draft: T.K., T.M.; Writing - review & editing: Y.W., T.K., T.M.; Visualization: T.K., T.M.; Supervision: T.M.; Project administration: T.M.; Funding acquisition: T.K., T.M.

Funding

This work was supported by a Ministry of Education, Culture, Sports, Science and Technology KAKENHI (22111006 to T.M.); by a Japan Society for the Promotion of Science (JSPS) KAKENHI (16H02457 to T.M.); by a Grant-in-Aid for JSPS Research Fellow (14J04218 to T.K.); by a JSPS KAKENHI (18K14837 to T.K.); and by the Mitsubishi Foundation (29147 to T.M.)

Supplementary information

Supplementary information available online at
http://dev.biologists.org/lookup/doi/10.1242/dev.162883.supplemental

References

Araki, K., Araki, M. and Yamamura, K. (2006). Negative selection with the Diphtheria toxin A fragment gene involves frequency of Cre-mediated cassette exchanges in ES cells. *J. Biochem.* **140**, 793-798.

Brockschnieder, D., Lappe-Siefke, C., Goebbels, S., Boesl, M. R., Nave, K.-A. and Riethmacher, D. (2004). Cell depletion due to diphtheria toxin fragment A after Cre-mediated recombination. *Mol. Cell. Biol.* **24**, 7636-7642.

Duronio, R., Bonnette, P. C. and O'Farrell, P. H. (1998). Mutations of the Drosophila dDP, dE2F, and cyclin E genes reveal distinct roles for the E2E-DP transcription factor and cyclin E during the G1-S transition. *Mol. Cell. Biol.* **18**, 141-151.

Estivill-Torrus, G., Pearson, H., van Heyningen, V. and Price, D. J. (2002). Pax6 is required to regulate the cell cycle and the rate of progression from symmetrical to asymmetrical division in mammalian cortical progenitors. *Development* **129**, 455-466.

Freret-Hodara, B., Cui, Y., Griveau, A., Vigier, L., Arai, Y., Touboul, J. and Pierani, A. (2017). Enhanced abventricular proliferation compensates cell death in the embryonic cerebral cortex. *Cereb. Cortex* **27**, 4701-4718.

Grosse, A. S., Pressprich, M. F., Curley, L. B., Hamilton, K. L., Morgolis, B., Hildebrand, J. D. and Gumucio, D. L. (2011). Cell dynamics in fetal intestinal epithelium: implications for intestinal growth and morphogenesis. *Development* **138**, 4423-4432.

Haubensak, W., Attardo, A., Denk, W. and Huttner, W. B. (2004). Neurons arise in the basal neuroepithelium of the early mammalian telencephalon: a major site of neurogenesis. *Proc. Natl. Acad. Sci. USA* **101**, 3196-3201.

Hevner, R. F., Hodge, R. D., Daza, R. A. M. and Englund, C. (2006). Transcription factors in glutamatergic neurogenesis: conserved programs in neocortex, cerebellum, and adult hippocampus. *Neurosci. Res.* **25**, 223-233.

Hu, D. J.-K., Baffet, A. D., Nayak, T., Akhmanova, A., Doye, V. and Vallee, R. B. (2013). Dynein recruitment to nuclear pores activates apical nuclear migration and mitotic entry in brain progenitor cells. *Cell* **154**, 1300-1313.

Ichikawa, T., Nakazato, K., Keller, P. J., Kajiura-Kobayashi, H., Stelzer, E. H., Mochizuki, A. and Nonaka, S. (2013). Live imaging of whole mouse embryos during gastrulation: migration analyses of epiblast and mesodermal cells. *PLoS ONE* **8**, e64506.

Katsuki, T., Ailani, D., Hiramoto, M. and Hiromi, Y. (2009). Intra-axonal patterning: intrinsic compartmentalization of the axonal membrane in *Drosophila* neurons. *Neuron* **64**, 188-199.

Kawaue, T., Sagou, K., Kiyonari, H., Ota, K., Okamoto, M., Shinoda, T., Kawaguchi, A. and Miyata, T. (2014). Neurogenin2-d4Venus and Gadd45g-d4Venus transgenic mice: visualizing mitotic and migratory behaviors of cells committed to the neuronal lineage in the developing mammalian brain. *Dev. Growth Differ.* **56**, 293-304.

Kosodo, Y. (2012). Interkinetic nuclear migration: beyond a hallmark of neurogenesis. *Cell. Mol. Life Sci.* **69**, 2727-2738.

Kosodo, Y., Suetsugu, T., Suda, M., Mimori-Kiyosue, Y., Toida, K., Baba, S. A., Kimura, A., and Matsuzaki, F. (2011). Regulation of interkinetic nuclear migration by cell cycle-coupled active and passive mechanisms in the developing brain. *EMBO J.* **30**, 1690-1704.

Lee, H. O. and Norden, C. (2013). Mechanisms controlling arrangements and movements of nuclei in pseudostratified epithelia. *Trend Cell Biol.* **23**, 141-150.

Leung, L., Klopper, A. V., Grill, S. W., Harris, W. A. and Norden, C. (2011). Apical migration of nuclei during G2 is a prerequisite for all nuclear motion in zebrafish neuroepithelia. *Development* **138**, 5003-5013.

Meyer, E. J., Ikmi, A. and Gibson, M. C. (2011). Interkinetic nuclear migration is a broadly conserved feature of cell division in pseudostratified epithelia. *Curr. Biol.* **21**, 485-491.

Miyata, T. (2008). Development of three-dimensional architecture of the neuroepithelium: role of pseudostratification and cellular 'community'. *Dev. Growth & Differ.* **50** Suppl.1, S105-S112.

Miyata, T., Kawaguchi, A., Okano, H. and Ogawa, M. (2001). Asymmetric inheritance of radial glial fibers by cortical neurons. *Neuron* **31**, 727-741.

Miyata, T., Kawaguchi, A., Saito, K., Kawano, M., Nuto, T. and Ogawa, M. (2004). Asymmetric production of surface-dividing and non-surface-dividing cortical progenitor cells. *Development* **131**, 3133-3145.

Miyata, T., Okamoto, M., Shinoda, T. and Kawaguchi, A. (2015). Interkinetic nuclear migration generates and opposes ventricular-zone crowding: insight into tissue mechanics. *Front. Cell. Neurosci.* **8**, 473.

Noctor, S. C., Martínez-Cerdeño, V., Ivic, L. and Kriegstein, A. R. (2004). Cortical neurons arise in symmetric and asymmetric division zones and migrate through specific phases. *Nat. Neurosci.* **7**, 136-144.

Norden, C. (2017). Pseudostratified epithelia - cell biology, diversity and roles in organ formation at a glance. *J. Cell Sci.* **130**, 1859-1863.

Ochiai, W., Nakatani, S., Takahara, T., Kainuma, M., Masaoka, M., Minobe, S., Namihira, M., Nakashima, K., Sakakibara, A., Ogawa, M. and Miyata, T. (2009). Periventricular Notch activation and asymmetric Ngn2 and Tbr2 expression in pair-generated neocortical daughter cells. *Mol. Cell. Neurosci.* **40**, 225-233.

Okamoto, M., Namba, T., Shinoda, T., Kondo, T., Watanabe, T., Inoue, Y., Takeuchi, K., Enomoto, Y., Ota, K., Oda, K. et al. (2013). TAG-1–assisted progenitor elongation streamlines nuclear migration to optimize subapical crowding. *Nat. Neurosci.* **16**, 1556-1566.

Reiner, O., Sapir, T. and Gerlitz, G. (2012). Interkinetic nuclear movement in the ventricular zone of the cortex. *J. Mol. Neurosci.* **46**, 516-526.

Sabherwal, N., Thuret, R., Lea, R., Stanley, P. and Papalopulu, N. (2014). aPKC phosphorylates p27Xic, providing a mechanistic link betwee apicobasal polarity and cell-cycle control. *Dev. Cell* **31**, 559-571.

Saito, K., Kawasoe, R., Sasaki, H., Kawaguchi, A. and Miyata, T. (2018). Neural progenitor cells undergoing Yap/Tead-mediated enhanced self-renewal form heterotopias more easily in the diencephalon than in the telencephalon. *Neurochem. Res.* **43**, 171-180.

Sakaue-Sawano, A., Kuroiwa, H., Morimura, T., Hanyu, A., Hama, H., Osawa, H., Kashiwagi, S., Fukami, K., Miyata, T., Miyoshi, H. et al. (2008). Visualizing spatiotemporal dynamics of multicellular cell-cycle progression. *Cell* **132**, 487-498.

Sapir, T., Sapoznik, S., Levy, T., Finkelshtein, D., Shmueli, A., Timm, T., Mandelkow, E.-M. and Reiner, O. (2008). Accurate balance of the polarity kinase MARK2/Par-1 is required for proper cortical neuronal migration. *J. Neurosci.* **28**, 5710-5720.

Sauer, F. C. (1935). Mitosis in the neural tube. *J. Comp. Neurol.* **62**, 377-405.

Schwab, M. H., Druffel-Augustin, S., Gass, P., Jung, M., Klugmann, M., Bartholomae, A., Rossner, M. J. and Nave, K.-A. (1998). Neuronal basic helix-loop-helix proteins (NEX, neuroD, NDRF): spatiotemporal expression and targeted disruption of the NEX gene in transgenic mice. *J. Neurosci.* **18**, 1408-1418.

Shinoda, T., Nagasaka, A., Inoue, Y., Higuchi, R., Minami, Y., Kato, K., Suzuki, M., Kondo, T., Kawaue, T., Saito, K. et al. (2018). Elasticity-based boosting of neuroepithelial nucleokinesis via indirect energy transfer from mother to daughter. *PLoS Biol.* **16**, e2004426.

Shoukimas, G. M. and Hinds, J. W. (1978). The development of the cerebral cortex in the embryoic mouse: an electron microscopic serial section analysis. *J. Comp. Neurol.* **179**, 795-830.

Spear, P. and Erickson, C. (2012). Interkinetic nuclear migration: a mysterious process in search of a function. *Dev. Growth. Differ.* **54**, 306-316.

Strzyz, P. J., Matejcic, M. and Norden, C. (2016). Heterogeneity, cell biology and tissue mechanics of pseudostratified epithelia: coordination of cell divisions and growth in tightly packed tissues. *Int. Rev. Cell. Mol. Biol.* **325**, 89-118.

Tabata, H. and Nakajima, K. (2003). Multipolar migration: the third mode of radial neuronal migration in the developing cerebral cortex. *J. Neurosci.* **23**, 9996-10001.

Takahashi, T., Nowakwski, R. S. and Caviness, V. S. Jr. (1996). Interkinetic and migratory behavior of a cohort of neocortical neurons arising in the early embryonic murine cerebral wall. *J. Neurosci.* **16**, 5762-5776.

Taverna, E. and Huttner, W. B. (2010). Neural progenitor nuclei in motion. *Neuron* **67**, 906-914.

Taverna, E., Götz, M. and Huttner, W. B. (2014). The cell biology of neurogenesis: toward an understanding of the development and evolution of the neocortex. *Annu. Rev. Cell. Dev. Biol.* **30**, 465-502.

Toma, K., Kumamoto, T. and Hanashima, C. (2014). The timing of upper-layer neurogenesis is conferred by sequential derepression and negative feedback from deep-layer neurons. *J. Neurosci.* **34**, 13259-13276.

Ueno, M., Katayama, K., Yamauchi, H., Nakayama, H. and Doi, K. (2006). Cell cycle progression is required for nuclear migration of neural progenitor cells. *Brain Res.* **1088**, 57-67.

Yamada, M., Udagawa, J., Hashimoto, R., Matsumoto, A., Hatta, T. and Otani, H. (2013). Interkinetic nuclear migration during early development of midgut and ureteric epithelia. *Anat. Sci. Int.* **88**, 31-37.

Yoshinaga, S., Ohkubo, T., Sasaki, S., Nuriya, M., Ogawa, Y., Yasui, M., Tabata, H. and Nakajima, K. (2012). A phosphatidylinositol lipids system, lamellipodin, and Ena/VASP regulate dynamic morphology of multipolar migrating cells in the developing cerebral cortex. *J. Neurosci.* **32**, 11643-11656.

Zecevic, N. (1993). Cellular composition of the telencephalic wall in human embryos. *Early Human Dev.* **32**, 131-149.